Simultaneous Schur Decomposition of Several Matrices to Achieve Automatic Pairing in Multidimensional Harmonic Retrieval Problems

Martin Haardt,[1] *Knut Hüper,*[1] *John B. Moore,*[2] *and Josef A. Nossek*[1]

1. Institute of Network Theory and Circuit Design
Technical University of Munich, D-80290 Munich, Germany

2. Department of Systems Engineering
Australian National University, Canberra ACT 0200, Australia

Phone: +49 (89) 289-28511, Fax: +49 (89) 289-68504
E-Mail: maha@nws.e-technik.tu-muenchen.de

***Abstract* — This paper presents a new Jacobi-type method to calculate a simultaneous Schur decomposition (SSD) of several real-valued, non-symmetric matrices by minimizing an appropriate cost function. Thereby, the SSD reveals the "average eigenstructure" of these non-symmetric matrices. This enables an R-dimensional extension of Unitary ESPRIT to estimate several undamped R-dimensional modes or frequencies along with their correct pairing in multidimensional harmonic retrieval problems. Unitary ESPRIT is an ESPRIT-type high-resolution frequency estimation technique that is formulated in terms of real-valued computations throughout. For each of the R dimensions, the corresponding frequency estimates are obtained from the real eigenvalues of a real-valued matrix. The SSD jointly estimates the eigenvalues of all R matrices and, thereby, achieves automatic pairing of the estimated R-dimensional modes via a closed-form procedure, that neither requires any search nor any other heuristic pairing strategy. Finally, we show how R-dimensional harmonic retrieval problems (with $R \geq 3$) occur in array signal processing and model-based object recognition applications.**

1. Introduction

Due to its simplicity and high-resolution capability, *ESPRIT* has become one of the most popular subspace-based direction of arrival or frequency estimation schemes. For certain array geometries, namely centro-symmetric arrays, or undamped modes, the computational complexity can be reduced significantly by formulating an ESPRIT-type algorithm in terms of real-valued computations throughout. The resulting algorithm is called *Unitary ESPRIT*, since the estimated phase factors are automatically constrained to the unit circle [5]. Furthermore, *Unitary ESPRIT* has recently been extended to the 2-D case to provide automatically paired azimuth and elevation angle estimates [8, 9, 14]. If, however, the carrier frequencies of the impinging wavefronts are no longer known (e.g., due to Doppler shifts) and may differ, the 2-D arrival angles, azimuth and elevation, and the corresponding carrier frequencies have to be estimated simultaneously. This model applies, for instance, to the surveillance radar system discussed in [13] and requires a 3-D extension of Unitary ESPRIT. Moreover, *3-D Unitary ESPRIT for joint 2-D angle and carrier estimation* can be used to determine the 2-D arrival angles, frequency offsets, and damping factors of the dominant multipaths in an SDMA (space division multiple access) mobile radio system.

Furthermore, the model-based object recognition scheme presented in [1] provides another application of the multidimensional harmonic retrieval problem. Here, the generated measurements correspond to samples from an R-dimensional lattice of sensors. Then, the estimated R-dimensional undamped modes are the parameters that reveal the object identity and pose.

This work was supported by the German Research Foundation (DFG) under contract number 322-730.

2. Multidimensional Harmonic Retrieval

Suppose we conduct N trials or experiments to observe R-dimensional data of the form $x_{k_1,k_2,\ldots,k_R}(n)$ for $1 \leq n \leq N$. The index of the rth dimension k_r is allowed to vary from 0 to $(M_r - 1)$ for $1 \leq r \leq R$. Thus, for fixed n, we have $M = \prod_{r=1}^{R} M_r$ different measurements of the data. This R-dimensional data consists of d undamped exponential modes in additive noise,

$$x_{k_1,k_2,\ldots,k_R}(n) = \sum_{i=1}^{d} \left(s_i(n) \prod_{r=1}^{R} e^{j\mu_i^{(r)} k_r} \right) + n_{k_1,k_2,\ldots,k_R}(n), \tag{1}$$

where the additive noise process is assumed to be zero-mean, *i.i.d.*, and uncorrelated with the signals. Here, we consider the task of estimating the d frequency vectors

$$\boldsymbol{\mu}_i = \left[\begin{array}{cccc} \mu_i^{(1)} & \mu_i^{(2)} & \ldots & \mu_i^{(R)} \end{array} \right]^T, \quad 1 \leq i \leq d, \tag{2}$$

that correspond to the d R-dimensional modes, and their correct pairing from the noise-corrupted measurements in (1).

3. Multidimensional Extension of Unitary ESPRIT

A very simple and efficient way to achieve this goal would be an R-dimensional extension of *Unitary ESPRIT*. As in the 1-D case [5], the algorithm is formulated in terms of real-valued computations throughout due to a bijective mapping between centro-Hermitian and real matrices [11], which automatically achieves forward-backward averaging of the data. After forming measurement vectors

$$\boldsymbol{x}(n) = \left[\begin{array}{c} x_{0,0,\ldots,0}(n) \\ x_{1,0,\ldots,0}(n) \\ \vdots \\ x_{M_1-1,0,\ldots,0}(n) \\ x_{M_1-1,1,\ldots,0}(n) \\ \vdots \\ x_{M_1-1,M_2-1,\ldots,M_R-2}(n) \\ x_{M_1-1,M_2-1,\ldots,M_R-1}(n) \end{array} \right] \in \mathbb{C}^M \tag{3}$$

from the scalar measurements in (1), the data matrix $\boldsymbol{X} \in \mathbb{C}^{M \times N}$ is constructed by taking N measurement vectors $\boldsymbol{x}(n), n = 1, 2, \ldots, N$, as its columns. If only a single vector $\boldsymbol{x}(n)$ is available ($N = 1$), an R-dimensional extension of the 2-D smoothing concept presented in [6] can be used to "create" more snapshots artificially.

Let us define left $\boldsymbol{\Pi}$-real matrices [11, 5] as matrices $\boldsymbol{Q} \in \mathbb{C}^{M \times M}$ satisfying $\boldsymbol{\Pi}_M \overline{\boldsymbol{Q}} = \boldsymbol{Q}$, where the overbar denotes complex conjugation without transposition. For any positive integer M, $\boldsymbol{I}_M$ denotes the identity matrix of size $M \times M$ and $\boldsymbol{\Pi}_M$ the $M \times M$ exchange

matrix with ones on its antidiagonal and zeros elsewhere. The unitary matrix

$$\boldsymbol{Q}_{2q+1} = \frac{1}{\sqrt{2}} \begin{bmatrix} \boldsymbol{I}_q & \boldsymbol{0} & \mathrm{j}\,\boldsymbol{I}_q \\ \boldsymbol{0}^T & \sqrt{2} & \boldsymbol{0}^T \\ \boldsymbol{\Pi}_q & \boldsymbol{0} & -\mathrm{j}\,\boldsymbol{\Pi}_q \end{bmatrix}, \tag{4}$$

for example, is left $\boldsymbol{\Pi}$-real of odd order. A unitary left $\boldsymbol{\Pi}$-real matrix of size $2q \times 2q$ is obtained from (4) by dropping its center row and center column. More left $\boldsymbol{\Pi}$-real matrices can be constructed by post-multiplying a left $\boldsymbol{\Pi}$-real matrix $\boldsymbol{Q}$ by an arbitrary real matrix $\boldsymbol{R}$, i.e., every matrix $\boldsymbol{Q}\,\boldsymbol{R}$ is left $\boldsymbol{\Pi}$-real.

In the first step of Unitary ESPRIT [8, 9, 14], forward-backward averaging is achieved by transforming the complex-valued data matrix $\boldsymbol{X}$ into the real-valued matrix[1]

$$\mathcal{T}(\boldsymbol{X}) = \boldsymbol{Q}_M^H \begin{bmatrix} \boldsymbol{X} & \boldsymbol{\Pi}_M\,\overline{\boldsymbol{X}}\,\boldsymbol{\Pi}_N \end{bmatrix} \boldsymbol{Q}_{2N} \in \mathbb{R}^{M \times 2N}.$$

Its d dominant left singular vectors $\boldsymbol{E}_s \in \mathbb{R}^{M \times d}$ are determined through a real-valued SVD of $\mathcal{T}(\boldsymbol{X})$ (square-root approach). Alternatively, they can be computed through a real-valued eigendecomposition of $\mathcal{T}(\boldsymbol{X})\mathcal{T}(\boldsymbol{X})^H \in \mathbb{R}^{M \times M}$ (covariance approach). Then, R real-valued invariance equations are formed,

$$\boldsymbol{K}_{(r)1}\boldsymbol{E}_s\boldsymbol{\Upsilon}_r \approx \boldsymbol{K}_{(r)2}\boldsymbol{E}_s \in \mathbb{R}^{m_r \times d}, \quad 1 \le r \le R, \tag{5}$$

where the R corresponding pairs of selection matrices are defined as

$$\begin{aligned} \boldsymbol{K}_{(r)1} &= 2 \cdot \mathrm{Re}\{\boldsymbol{Q}_{m_r}^H \boldsymbol{J}_{(r)2}\,\boldsymbol{Q}_M\} \\ \boldsymbol{K}_{(r)2} &= 2 \cdot \mathrm{Im}\{\boldsymbol{Q}_{m_r}^H \boldsymbol{J}_{(r)2}\,\boldsymbol{Q}_M\}. \end{aligned}$$

Here, the matrices $\boldsymbol{J}_{(r)2}$ of size $m_r \times M$ are given by

$$\boldsymbol{J}_{(r)2} = \boldsymbol{I}_{M_R} \otimes \boldsymbol{I}_{M_{R-1}} \otimes \ldots \otimes \boldsymbol{I}_{M_{r+1}} \otimes \boldsymbol{J}_2^{(M_r)} \otimes \boldsymbol{I}_{M_{r-1}} \otimes \ldots \otimes \boldsymbol{I}_{M_1},$$

where $\otimes$ denotes the Kronecker matrix product,

$$m_r = \frac{M(M_r - 1)}{M_r}, \quad \text{and} \quad \boldsymbol{J}_2^{(M_r)} = (M_r - 1) \begin{bmatrix} 1 & (M_r - 1) \\ \boldsymbol{0} & \boldsymbol{I}_{M_r - 1} \end{bmatrix}.$$

The R invariance equations (5) are solved independently via least squares or total least squares or jointly via an R-dimensional extension of structured least squares [7], yielding R real-valued matrices $\boldsymbol{\Upsilon}_r \in \mathbb{R}^{d \times d}$, $1 \le r \le R$. Note that these matrices are not necessarily symmetric.

In the noiseless case or with an infinite number of experiments N, the R solutions $\boldsymbol{\Upsilon}_r$ of (5) have real-valued eigenvalues and share the same set of real-valued eigenvectors. More specifically, they admit the following eigendecompositions

$$\boldsymbol{\Upsilon}_r = \boldsymbol{T}\,\boldsymbol{\Omega}_r\,\boldsymbol{T}^{-1} \quad \text{with} \quad \boldsymbol{\Omega}_r = \mathrm{diag}\left\{ \tan\left(\frac{\mu_i^{(r)}}{2} \right) \right\}_{i=1}^{d}, \tag{6}$$

$1 \le r \le R$. Notice first that all the matrices in (6) are real-valued. Secondly, the eigenvalues of $\boldsymbol{\Upsilon}_r$, i.e., the diagonal elements of $\boldsymbol{\Omega}_r$, contain the desired frequency information. Thirdly, if the matrix of eigenvectors $\boldsymbol{T} \in \mathbb{R}^{d \times d}$ in the spectral decompositions of $\boldsymbol{\Upsilon}_r$ is the same for all $r, 1 \le r \le R$, the diagonal elements of the matrices $\boldsymbol{\Omega}_r$ and, therefore, also the desired frequencies in (2) are automatically paired.

In practice, though, only a finite number N of noise-corrupted experiments (or measurements) is available. Therefore, the R matrices $\boldsymbol{\Upsilon}_r$ do not exactly share the same set of eigenvectors. To determine the set of eigenvectors only from one of the $\boldsymbol{\Upsilon}_r$ is, obviously, not the best solution, since this strategy would rely on an arbitrary choice and would also discard information contained in the other $R - 1$ matrices. Moreover, each of the $\boldsymbol{\Upsilon}_r$ might have some degenerate (multiple) eigenvalues, while the whole set $\boldsymbol{\Upsilon}_r$, $1 \le r \le R$, has well determined common eigenvectors $\boldsymbol{T}$ (for $N \to \infty$ or $\sigma_N^2 \to 0$). Thus, from a statistical point of view, it is desirable, for the sake of accuracy and robustness, to compute the "average eigenstructure" of these matrices [3]. In the 2-D case, automatic pairing can be achieved by calculating the eigenvalues of the "complexified" matrix $\boldsymbol{\Upsilon}_1 + \mathrm{j}\,\boldsymbol{\Upsilon}_2 \in \mathbb{C}^{d \times d}$, cf. the derivation of 2-D Unitary ESPRIT in [8, 9, 14]. If, however, $R > 2$, this "trick" has to be extended to the R-dimensional case. To this end, we will present a Jacobi-type method to calculate a simultaneous Schur decomposition (SSD) of several matrices.

4. Simultaneous Schur Decomposition (SSD)

4.1. Minimization Task

Recall that the eigenvalues of real-valued non-symmetric matrices can efficiently be computed through an eigenvalue-revealing real Schur decomposition [4]. In the noiseless case or with an infinite number of experiments N, the new SSD of the R matrices $\boldsymbol{\Upsilon}_r$, $1 \le r \le R$, yields R (real-valued) upper triangular matrices that exhibit the automatically paired eigenvalues on their main diagonals. Under the assumption of additive noise and a finite number of experiments N, an orthogonal similarity transformation might not be able to produce R upper triangular matrices simultaneously, since the R "noisy" matrices do not share a common set of eigenvectors. In this case, the resulting matrices should be "almost" upper triangular in a least squares sense as explained in the sequel.

To derive an appropriate algorithm, let $\mathcal{L}(\boldsymbol{\Upsilon}_r)$ denote an operator that extracts the strictly lower triangular part of its matrix-valued argument by setting the upper triangular part and the elements on the main diagonal to zero. Then, we want to minimize the cost function

$$\psi(\boldsymbol{\Theta}) = \sum_{r=1}^{R} \left\| \mathcal{L}(\boldsymbol{\Theta}^T \boldsymbol{\Upsilon}_r \boldsymbol{\Theta}) \right\|_{\mathrm{F}}^2 \tag{7}$$

over the set of all orthogonal matrices $\boldsymbol{\Theta}$ of size $d \times d$. As usual, $\|\cdot\|_{\mathrm{F}}$ denotes the Frobenius-norm.[2]

4.2. Jacobi-Type Algorithm

In Jacobi-type algorithms, the orthogonal matrix $\boldsymbol{\Theta}$ is decomposed into a product of elementary Jacobi rotations

$$\boldsymbol{\Theta}_{qp} = \begin{bmatrix} 1 & \cdots & 0 & \cdots & 0 & \cdots & 0 \\ \vdots & \ddots & \vdots & & \vdots & & \vdots \\ 0 & \cdots & c & \cdots & s & \cdots & 0 \\ \vdots & & \vdots & \ddots & \vdots & & \vdots \\ 0 & \cdots & -s & \cdots & c & \cdots & 0 \\ \vdots & & \vdots & & \vdots & \ddots & \vdots \\ 0 & \cdots & 0 & \cdots & 0 & \cdots & 1 \end{bmatrix} \tag{8}$$

[1] If the the left $\boldsymbol{\Pi}$-real matrices $\boldsymbol{Q}_M$ and $\boldsymbol{Q}_{2N}$ are chosen according to (4) and M is even, an efficient computation of the transformation $\mathcal{T}(\boldsymbol{X}) \in \mathbb{R}^{M \times 2N}$ from the complex-valued data matrix $\boldsymbol{X}$ only requires $M \cdot 2N$ real additions and no multiplication [5].

[2] If all the $\boldsymbol{\Upsilon}_r$ were symmetric, the minimization of (7) would achieve an approximate simultaneous *diagonalization* of these matrices. An efficient Jacobi-type technique to achieve such an approximate simultaneous diagonalization has been presented in [2, 3]. This algorithm, however, is not applicable in our case, since the $\boldsymbol{\Upsilon}_r$ are not symmetric. Therefore, the minimization of the sum of the off-diagonal norms of these R matrices via a sequence of simultaneous orthogonal transformations as discussed in [2, 3] would not reveal the desired "average eigenstructure" of these non-symmetric matrices.

such that

$$\mathbf{\Theta} = \prod_{\#\text{ of sweeps}} \prod_{q=1}^{d} \prod_{p=1}^{q-1} \mathbf{\Theta}_{qp}. \tag{9}$$

Jacobi rotations $\mathbf{\Theta}_{qp}$ are defined as orthogonal matrices where all diagonal elements are 1 except for the two elements c in rows (and columns) p and q. Likewise, all off-diagonal elements of $\mathbf{\Theta}_{qp}$ are 0 except for the two elements s and $-s$, cf. (8). The real numbers $c = \cos\vartheta$ and $s = \sin\vartheta$ are the cosine and sine of a rotation angle ϑ. In the sequel, we describe a procedure to choose the rotation angle ϑ at a particular iteration such that the cost function $\psi(\mathbf{\Theta})$ is decreased as much as possible. To this end, observe that, at each iteration, the R real-valued matrices $\mathbf{\Upsilon}_r$ are transformed according to

$$\mathbf{\Upsilon}'_r = \mathbf{\Theta}_{qp}^T \mathbf{\Upsilon}_r \mathbf{\Theta}_{qp}, \quad 1 \le r \le R. \tag{10}$$

It is easily seen that the orthogonal transformation (10) changes only elements of $\mathbf{\Upsilon}_r$ that appear in rows and columns p and q. More specifically, the entries of $\mathbf{\Upsilon}'_r$ changed on its strictly lower triangular part $\mathcal{L}(\mathbf{\Upsilon}'_r)$ are given by

$$\begin{aligned}
\upsilon_{pk}^{(r)\prime} &= c\upsilon_{pk}^{(r)} - s\upsilon_{qk}^{(r)}, \qquad 1 \le k < p \\
\upsilon_{qk}^{(r)\prime} &= s\upsilon_{pk}^{(r)} + c\upsilon_{qk}^{(r)}, \qquad 1 \le k < q, \qquad k \ne p \\
\upsilon_{qp}^{(r)\prime} &= s(c\upsilon_{pp}^{(r)} - s\upsilon_{pq}^{(r)}) + c(c\upsilon_{qp}^{(r)} - s\upsilon_{qq}^{(r)}) \\
\upsilon_{kp}^{(r)\prime} &= c\upsilon_{kp}^{(r)} - s\upsilon_{kq}^{(r)}, \qquad p < k \le d, \qquad k \ne q \\
\upsilon_{kq}^{(r)\prime} &= s\upsilon_{kp}^{(r)} + c\upsilon_{kq}^{(r)}, \qquad q < k \le d.
\end{aligned}$$

Here, $\upsilon_{k\ell}^{(r)}$ and $\upsilon_{k\ell}^{(r)\prime}$ denote the (k,ℓ)-entries of the matrices $\mathbf{\Upsilon}_r$ and $\mathbf{\Upsilon}'_r$, respectively. Recall that only $\mathcal{L}(\mathbf{\Upsilon}'_r)$ contributes to the cost function (7). Therefore, the change of this cost function can be expressed as

$$\begin{aligned}
\Delta\psi(\mathbf{\Theta}_{qp}) &= \sum_{r=1}^{R} \left(\left\| \mathcal{L}(\mathbf{\Upsilon}'_r) \right\|_{\mathrm{F}}^2 - \left\| \mathcal{L}(\mathbf{\Upsilon}_r) \right\|_{\mathrm{F}}^2 \right) \qquad (11) \\
&= \sum_{r=1}^{R} \left(\upsilon_{qp}^{(r)\prime 2} + \sum_{k=(p+1)}^{q-1} \left(\upsilon_{qk}^{(r)\prime 2} + \upsilon_{kp}^{(r)\prime 2} \right) \right. \\
&\quad \left. - \upsilon_{qp}^{(r)2} - \sum_{k=(p+1)}^{q-1} \left(\upsilon_{qk}^{(r)2} + \upsilon_{kp}^{(r)2} \right) \right),
\end{aligned}$$

where we have used the fact that

$$\upsilon_{pk}^{(r)\prime 2} + \upsilon_{qk}^{(r)\prime 2} = \upsilon_{pk}^{(r)2} + \upsilon_{qk}^{(r)2}, \quad 1 \le k < p,$$

$$\text{and} \quad \upsilon_{kp}^{(r)\prime 2} + \upsilon_{kq}^{(r)\prime 2} = \upsilon_{kp}^{(r)2} + \upsilon_{kq}^{(r)2}, \quad q < k \le d.$$

Differentiating (11) with respect to ϑ, using the abbreviation $t = \tan\vartheta$ which implies $c = \cos\vartheta = 1/\sqrt{1+t^2}$, $s = \sin\vartheta = t/\sqrt{1+t^2}$, and multiplying the result by $(1+t^2)^2/2$, yields the fourth order polynomial

$$p(t) = \begin{bmatrix} 1 & t & t^2 & t^3 & t^4 \end{bmatrix} \cdot \sum_{r=1}^{R} \boldsymbol{c}^{(r)} \tag{12}$$

$$\text{with} \quad \boldsymbol{c}^{(r)} = \boldsymbol{c}_{qp}^{(r)} + \sum_{k=(p+1)}^{q-1} \left(\boldsymbol{c}_{\text{add}}(\upsilon_{pk}^{(r)}, \upsilon_{qk}^{(r)}) - \boldsymbol{c}_{\text{add}}(\upsilon_{kp}^{(r)}, \upsilon_{kq}^{(r)}) \right),$$

$$\boldsymbol{c}_{qp}^{(r)} = \begin{bmatrix} \upsilon_{qp}^{(r)} \cdot (\upsilon_{pp}^{(r)} - \upsilon_{qq}^{(r)}) \\ (\upsilon_{pp}^{(r)} - \upsilon_{qq}^{(r)})^2 - 2\upsilon_{qp}^{(r)} \cdot (\upsilon_{pq}^{(r)} + \upsilon_{qp}^{(r)}) \\ -3 \cdot (\upsilon_{pp}^{(r)} - \upsilon_{qq}^{(r)}) \cdot (\upsilon_{pq}^{(r)} + \upsilon_{qp}^{(r)}) \\ -(\upsilon_{pp}^{(r)} - \upsilon_{qq}^{(r)})^2 + 2\upsilon_{pq}^{(r)} \cdot (\upsilon_{pq}^{(r)} + \upsilon_{qp}^{(r)}) \\ \upsilon_{pq}^{(r)} \cdot (\upsilon_{pp}^{(r)} - \upsilon_{qq}^{(r)}) \end{bmatrix},$$

$$\text{and} \quad \boldsymbol{c}_{\text{add}}(a,b) = \begin{bmatrix} a \cdot b & a^2 - b^2 & 0 & a^2 - b^2 & -a \cdot b \end{bmatrix}^T.$$

The critical points of $\Delta\psi(\mathbf{\Theta}_{qp})$ in (11) are the roots of the polynomial $p(t)$ in (12). If the coefficient of t^4 in (12), i.e., the last component of the coefficient vector $\sum_{r=1}^{R} \boldsymbol{c}^{(r)}$, equals zero, $p(t)$ reduces to a third order polynomial. Then, $t = \infty$ is also a critical point[3] of $\Delta\psi(\mathbf{\Theta}_{qp})$. Notice that only the real-valued roots of the polynomial $p(t)$ in (12) yield valid options for the desired orthogonal rotation $\mathbf{\Theta}_{qp}$. From these possibilities, we choose the the value of t (or the corresponding rotation angle ϑ) that minimizes (11). However, we only use the corresponding elementary Jacobi rotation $\mathbf{\Theta}_{qp}$ if

$$\Delta\psi(\mathbf{\Theta}_{qp}) < 0,$$

i.e., the chosen rotation reduces the cost function. Otherwise, no rotation is applied as this particular iteration step. Such a strategy is closely related to the one-dimensional Jacobi-type methods discussed in [10].

5. 3-D Unitary ESPRIT for Joint 2-D Angle and Carrier Estimation

As a 3-D application of the new simultaneous Schur decomposition (SSD), consider a uniform rectangular array consisting of $M_1 \times M_2$ identical antennas lying on a rectangular grid in the x-y plane. The inter-element spacing in x- and y-direction will be called Δ_x and Δ_y, respectively. Incident on the array are d narrowband planar

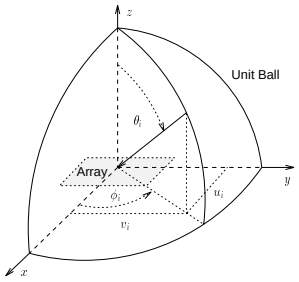

Figure 1: Definitions of azimuth ($-180^\circ < \phi_i \le 180^\circ$) and elevation ($0^\circ \le \theta_i \le 90^\circ$)

wavefronts with speed of propagation c, azimuth ϕ_i, elevation θ_i, and carrier frequency f_i, $1 \le i \le d$. Let $u_i = \cos\phi_i \sin\theta_i$ and $v_i = \sin\phi_i \sin\theta_i$ denote the direction cosines of the ith source relative to the x- and y-axes, respectively (Fig. 1). For each source,

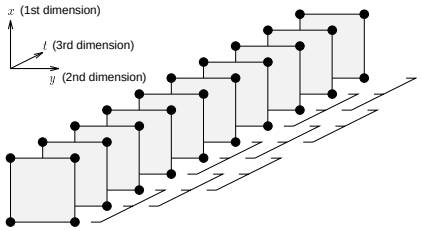

Figure 2: 3-D Unitary ESPRIT for joint 2-D angle and carrier estimation using a URA of 2×2 elements and $M_3 = 10$ (temporal) snapshots. Temporal smoothing with $L = L_3 = 8$ subarrays, each containing $M_{\text{sub}3} = M_3 - L_3 + 1 = 3$ snapshots, is performed along the third (the temporal) dimension.

the two-dimensional angular position and the corresponding carrier frequency have to be estimated simultaneously. If M_3 snapshots are observed at each sensor, 3-D Unitary ESPRIT with SSD can handle

[3] Obviously, $t = \infty$ corresponds to the rotation angle $\vartheta = \pi/2$. Alternatively, one could consider $t = -\infty$. Notice that $t = \infty$ and $t = -\infty$ lead to the same change of the cost function (11).

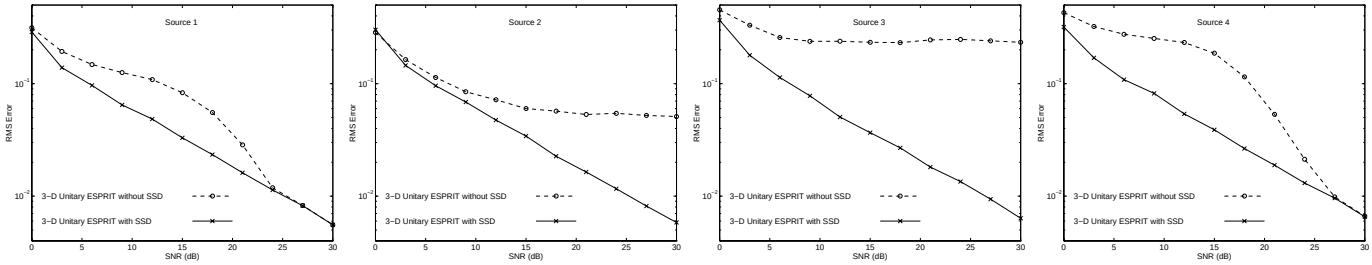

Figure 3: Comparison of 3-D Unitary ESPRIT with and without the simultaneous Schur decomposition (SSD). Temporal smoothing with 8 subarrays was performed along the third (the temporal) dimension ($d = 4$, $R = 3$, $M_1 = 2$, $M_2 = 2$, $M_3 = 10$, $N = 1$, $T = 500$ trials).

this task. In this case, $N = 1$, and the $R = 3$ dimensional frequency vectors (2) have the components

$$\mu_i^{(1)} = \frac{2\pi f_i}{c}\Delta_x u_i, \quad \mu_i^{(2)} = \frac{2\pi f_i}{c}\Delta_y v_i, \quad \text{and} \quad \mu_i^{(3)} = 2\pi f_i T_s,$$

where T_s denotes the sampling interval. Since only one experiment ($N = 1$) is available, smoothing should be used as a preprocessing step. In most applications, it fairly easy to collect a large number of temporal snapshots M_3, whereas increasing the number of sensors in either the x- or the y-direction (M_1 or M_2) would be significantly more expensive. We, therefore, suggest to use smoothing only along the third (the temporal) dimension as illustrated in Fig. 2.

Simulations were conducted with $d = 4$ uncorrelated wavefronts and the following parameters: $M_1 = 2$, $M_2 = 2$, $M_3 = 10$,

$$\boldsymbol{\mu}_1 = \pi[\ 0.05 \quad -0.5 \quad 0.8\ ]^T, \quad \boldsymbol{\mu}_2 = \pi[\ 0.5 \quad 0.5 \quad 0.8\ ]^T,$$
$$\boldsymbol{\mu}_3 = \pi[\ 0.5 \quad 0.5 \quad 0.2\ ]^T, \quad \boldsymbol{\mu}_4 = \pi[\ 0.0 \quad 0.2 \quad 0.2\ ]^T.$$

Temporal smoothing with 8 subarrays, each containing 3 snapshots, was performed along the third (the temporal) dimension, cf. Fig. 2. As an *ad hoc* alternative to the SSD, we have also computed the eigendecomposition of $\boldsymbol{\Upsilon}_1$ and applied the resulting eigenvectors to $\boldsymbol{\Upsilon}_2$ and $\boldsymbol{\Upsilon}_3$ as suggested for the 2-D case in [12]. Let $\hat{\boldsymbol{\mu}}_{i_k} \in \mathbb{R}^3$ denote the estimated frequency vector of the ith source obtained at the kth run. Sample performance statistics were computed from $T = 500$ independent trials as

$$\text{RMSE}_i = \sqrt{\frac{1}{T}\sum_{k=1}^{T}\left\|\frac{1}{\pi}\left(\hat{\boldsymbol{\mu}}_{i_k} - \boldsymbol{\mu}_i\right)\right\|^2},$$

$i = 1, 2, 3, 4$. The resulting RMS errors for sources 1, 2, 3, and 4 are depicted in Fig. 3, which clearly illustrates that the SSD outperforms the *ad hoc* approach (3-D Unitary ESPRIT without SSD). Using the same parameters as before, we have also plotted the evolution of the cost function $\psi(\boldsymbol{\Theta})$, defined in (7), for different SNRs (Fig. 4). As expected, the value of the cost function at convergence indicates the strength of the additive noise. Only without additive noise, the three matrices $\boldsymbol{\Upsilon}_r$, $r = 1, 2, 3$, share precisely the same eigenvectors, and the cost function $\psi(\boldsymbol{\Theta})$ can, therefore, be driven to zero.

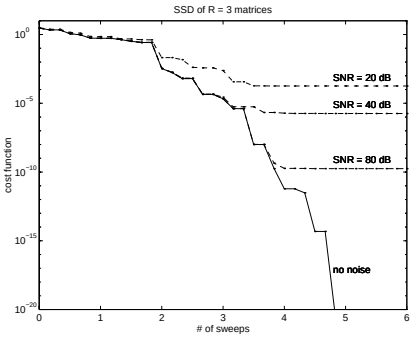

Figure 4: Evolution of the cost function $\psi(\boldsymbol{\Theta})$ for different SNRs ($d = 4$, $R = 3$, $M_1 = 2$, $M_2 = 2$, $M_3 = 10$, $N = 1$)

References

[1] J. Byrne, D. Cyganski, R. Vaz, and C. R. Wright, "An N-D technique for coherent wave DOA estimation", in *Proc. 7th SP Workshop on Statistical Signal Processing*, pp. 425–428, Quebec City, Canada, June 1994.

[2] J. F. Cardoso and A. Souloumiac, "Blind beamforming for non Gaussian signals", *IEE Proc.-F*, vol. 140, no. 6, pp. 362–370, Dec. 1993.

[3] J. F. Cardoso and A. Souloumiac, "Jacobi angles for simultaneous diagonalization", *SIAM J. Matrix Anal. Appl.*, vol. 17, pp. 161–164, Jan. 1996.

[4] G. H. Golub and C. F. van Loan, *Matrix Computations*, Johns Hopkins University Press, Baltimore, MD, 2nd edition, 1989.

[5] M. Haardt and J. A. Nossek, "Unitary ESPRIT: How to obtain increased estimation accuracy with a reduced computational burden", *IEEE Trans. Signal Processing*, vol. 43, pp. 1232–1242, May 1995.

[6] M. Haardt and J. A. Nossek, "2-D spatial filters for coherent multipath signals", in *Proc. IEEE / IEE Int. Conf. on Telecommunications*, B. Sankur, Ed., vol. 2, pp. 675–678, Istanbul, Turkey, Apr. 1996.

[7] M. Haardt and J. A. Nossek, "Structured least squares to improve the performance of ESPRIT-type high-resolution techniques", in *Proc. IEEE Int. Conf. Acoust., Speech, Signal Processing*, Atlanta, GA, May 1996, to be published.

[8] M. Haardt, M. D. Zoltowski, C. P. Mathews, and J. A. Nossek, "2D Unitary ESPRIT for efficient 2D parameter estimation", in *Proc. IEEE Int. Conf. Acoust., Speech, Signal Processing*, vol. 3, pp. 2096–2099, Detroit, MI, May 1995.

[9] M. Haardt, M. D. Zoltowski, C. P. Mathews, and J. Ramos, "ESPRIT and closed-form 2-D angle estimation with planar arrays", in *The Digital Signal Processing Handbook*, V. K. Madisetti and D. B. Williams, Eds. CRC Press and IEEE Press, 1996, scheduled to appear.

[10] K. Hüper and U. Helmke, "Structure and convergence of Jacobi-type methods", Tech. Rep. TUM-LNS-TR-95-2, Technical University of Munich, Institute of Network Theory and Circuit Design, July 1995, submitted to *Numerische Mathematik*.

[11] A. Lee, "Centrohermitian and skew-centrohermitian matrices", *Linear Algebra and its Applications*, vol. 29, pp. 205–210, 1980.

[12] A. J. van der Veen, P. B. Ober, and E. F. Deprettere, "Azimuth and elevation computation in high resolution DOA estimation", *IEEE Trans. Signal Processing*, vol. 40, pp. 1828–1832, July 1992.

[13] F. Vanpoucke, *Algorithms and Architectures for Adaptive Array Signal Processing*, Ph. D. dissertation, Katholieke Universiteit Leuven, Leuven, Belgium, Feb. 1995.

[14] M. D. Zoltowski, M. Haardt, and C. P. Mathews, "Closed-form 2D angle estimation with rectangular arrays in element space or beamspace via Unitary ESPRIT", *IEEE Trans. Signal Processing*, vol. 44, Feb. 1996, scheduled to appear.